

Critical quasielastic light scattering in $\text{KTa}_{0.968}\text{Nb}_{0.032}\text{O}_3$

Edward Lee and L. L. Chase

Physics Department, Indiana University, Bloomington, Indiana 47405

L. A. Boatner

Solid State Division, Oak Ridge National Laboratory, Oak Ridge, Tennessee 37830

(Received 22 August 1984)

Intense quasielastic light scattering is observed in potassium tantalate niobate at temperatures near the ferroelectric transition at $T_c \sim 40$ K. The central peak (CP) has a non-Lorentzian shape and consists of a sharp component with a broad tail. Near T_c , the sharp component narrows to 1.5 GHz (half-width at half maximum) which is close to the limit of resolution achievable when using an I_2 vapor filter to eliminate elastically scattered light. It is, therefore, possible that the CP has a much narrower distribution than that of the renormalized Fabry-Perot data. Spectra obtained over a range of frequency shifts including the Raman scattering from the soft TO mode have been fitted by a coupled-mode formalism in which it is assumed that the CP derives all of its intensity from the coupling to the TO phonon. This model accounts reasonably well for the relative intensities of the CP and phonon and the large renormalized frequency of the phonon near T_c . The integrated intensity of the CP has a temperature dependence which is singular at T_c , whereas that of the TO phonon is close to a step-function increase at T_c . Although ordinary two-phonon difference (phonon-density-fluctuations) scattering cannot be excluded as a possible origin of the observed quasielastic scattering, several properties of the quasielastic and Raman spectra, as well as other recent experimental results, suggest a mechanism involving fluctuations due to the disorder in the polarizabilities and force constants introduced by the Nb substitution.

I. INTRODUCTION

The dynamical behavior of crystalline solids near second-order phase transitions has been a subject of great interest for well over a decade. A striking experimental manifestation of this behavior is the occurrence of central peaks (CP's) that reflect relaxational responses of the media, distinct from the coexisting, damped periodic responses inherent in the soft phonon or magnon modes. In the case of nominally displacive structural transitions, the coupling between the soft phonon mode and the central-peak fluctuations leads to a saturation of the soft-mode frequency at a nonzero value near T_c , and the dynamical features of the transition become dominated by the fluctuation processes which produce the central peak. Both intrinsic and impurity or defect-induced mechanisms involving coupling to the order parameter of the transition have been proposed in order to account for these quasielastic peaks.¹ In a majority of experimental investigations of displacive transitions, the observed frequency distribution of the CP is too narrow to be accounted for by known intrinsic mechanisms, and the influence of relatively slowly relaxing or static impurities and defects is likely. Relatively few investigations of fluctuations associated with known and well-characterized defects have been reported,²⁻¹⁰ however, and none of these have directly observed the dynamical behavior resulting from the coupling of the defects with the soft mode.

There have been numerous theoretical treatments of the effects of impurities coupled linearly or quadratically with the soft-mode order parameter.¹¹ These effects vary con-

siderably with the classification¹² of the defect according to the type and strength of its coupling to the order parameter, as well as its dynamical properties (i.e., frozen or reorienting, "quenched" or mobile, etc.). At the present time quantitative predictions concerning the influence of defects on phase transitions are only available for very small defect concentrations where a mean-field (MFT) treatment is applicable.^{12,13} The effects of defects on the critical behavior have not yet been thoroughly elucidated, but for quenched defects, modified static¹⁴ and dynamic¹⁵ critical behavior is expected.

Mixed-crystal systems which undergo phase transitions provide an excellent opportunity to examine the influence of impurities over a very wide range of concentrations. When the concentrations of the minority and majority constituents become comparable, the resulting disordered systems can exhibit either sharp or diffuse transitions to phases that are often not well characterized as either ordered or glasslike. A particularly interesting material for further experimental work in this area is the cubic perovskite KTaO_3 , which is an incipient ferroelectric. The substitutions of Nb for Ta and of Na or Li for K lead to ferroelectric phase transitions. KTN ($\text{KTa}_{1-x}\text{Nb}_x\text{O}_3$) is an extensively studied member of this class of mixed crystals.¹⁶ For $x \gtrsim 0.04$ successive transitions to ferroelectric phases of tetragonal, orthorhombic, and rhombohedral symmetry occur with decreasing temperature. For $0.008 \lesssim x \lesssim 0.04$ a single, second-order transition occurs from the cubic phase to a presumed rhombohedral phase. Raman scattering studies in these samples show the presence of a single soft TO phonon whose frequency

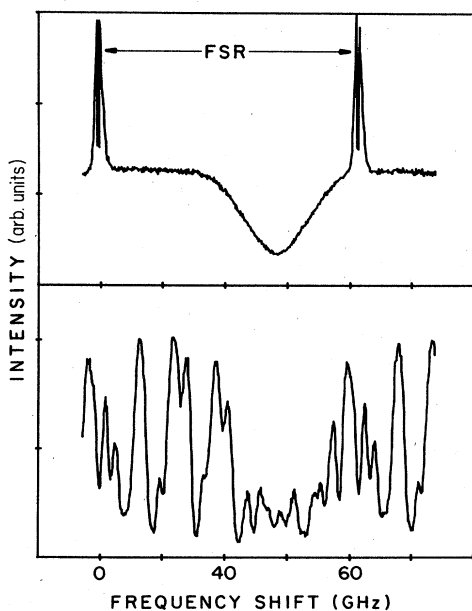


FIG. 1. Upper trace: Transmission of Fabry-Perot interferometer and double monochromator. The sharp feature folded back on scale is injected 5154-Å laser light. Lower trace: I_2 filter is inserted between the interferometer and monochromator.

ω_{TO} remains finite at T_c . Furthermore, $\omega_{TO}(T_c)$ increases with increasing Nb concentration.¹⁶ This latter result suggests the possibility of a coupling to the soft mode to fluctuations involving the disorder introduced by the Nb ions.

In the present work, the low-frequency dynamics of a KTN sample with $x=0.032$ have been examined by means of Fabry-Perot spectroscopy. An intense quasielastic peak strongly coupled to the soft TO vibrational mode has been observed. This CP has a non-Lorentzian shape and a singular increase in its integrated intensity near $T_c=39$ K. Measurements over a frequency interval including the scattering from the soft TO phonon show that the behavior of the joint scattering spectrum can be adequately accounted for by the coupling of the phonon to the fluctuations responsible for the CP.

II. EXPERIMENTAL METHODS

All the results reported here were obtained on one flux-grown sample of KTN with $x=0.032$. This sample was selected for its good optical homogeneity in the cubic phase. Similar, but less extensive, observations of quasielastic scattering were made in two other samples with niobium concentrations in the range of 2–3 mol %. Although sample heating resulting from a slight absorption of the laser light in these other samples caused some uncertainty in the temperature in the focal region, the behavior of the spectra was very similar to that of the sample chosen for extensive study. We believe that the properties reported here are not significantly sample dependent. The sample was cut and polished with faces perpendicular to the $\langle 111 \rangle$, $\langle 1\bar{1}0 \rangle$, and $\langle 11\bar{2} \rangle$ directions, which are one possible set of principal axes in the rhombohedral phase. Attempts were made to pole the sample

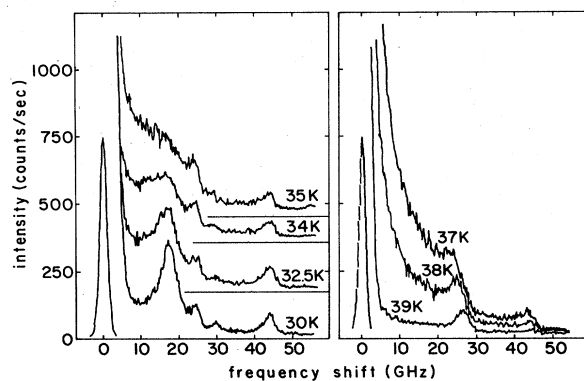


FIG. 2. Brillouin and quasielastic spectra observed without I_2 filter. T_c is at 37.5 K.

below T_c with electric fields up to 3 kV/cm along the $\langle 111 \rangle$ polar axis. This procedure resulted in a reduction of the number of Brillouin components below T_c to the number expected for a single domain. There was, however, nearly complete depolarization of the exciting laser beam, initially polarized along $\langle 111 \rangle$, after passage through the sample. It is possible that this depolarization results from a surface layer which is not a single domain, or from another surface phase.¹⁷ Presumably the same effect also occurs for the scattered light; in fact, the observed spectra were found to have little or no dependence on the polarizations of either the laser or of the scattered light. For this reason, no polarization data were obtained.

The sample was enclosed in a copper holder, to which it was bonded with General Electric type 7031 varnish. The holder had small apertures for optical access and a heater and thermocouple, bonded near the sample, for temperature regulation to better than 0.1 K in an environment of He exchange gas cooled by liquid He. The silver electrodes that were used for poling the sample were also employed to measure the dielectric constant at 1 kHz. These latter measurements gave broad maxima, presumably because of a distribution of values of T_c of several degrees kelvin over the volume of the sample. No exact correspondence was possible with the very small (~ 50 μm) dimensions probed by the light scattering optics.

The quasielastic scattering was analyzed by a computer-stabilized-and-controlled, triple-pass, Fabry-Perot (FP) interferometer with a free-spectral range (FSR) of 83 GHz and a resolution of 1.6 GHz. A double grating monochromator was used as a narrow bandpass filter on the output of the interferometer. This monochromator rejected scattered light outside a portion of the free-spectral range of the interferometer centered on the Stokes side of the laser wavelength. It was also of importance in correcting for the iodine filter absorption discussed below. The output of the monochromator was detected by a photomultiplier tube, photon-counting electronics, and a computer data acquisition system.

A molecular iodine filter¹⁸ was used at the output of the FP in order to reject elastically scattered light. The Ar excitation laser, operating near 5145 Å, was tuned to a strong absorption dip of I_2 vapor. It is well known that the I_2 filter blocks a frequency region about 1 GHz wide

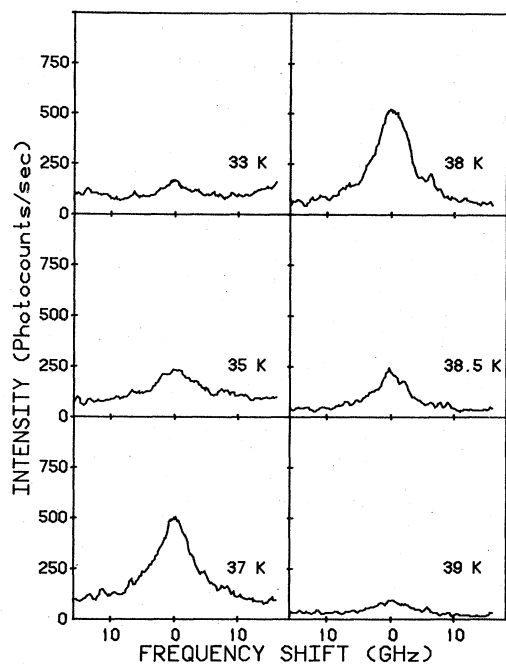


FIG. 3. Central-peak spectra reconstructed from measurements with I_2 filter. T_c is at 38 K.

centered at the laser line and introduces a considerable amount of other structure into the scattered light spectrum.¹⁸⁻²⁰ Digital renormalization techniques can recover some, but not all, of the scattered light spectrum for spectral features that are wider than the absorption notches of the filter.^{19,20} The normalization procedure used in this work involves the passage through the system of white light from a tungsten source. The transmission function with and without the I_2 filter is shown schematically in Fig. 1. The rounded trapezoidal response is that of the double monochromator, with a passband somewhat less than the FSR of the FP. The data are corrected for the transmission functions of both the monochromator and filter by dividing each data point by the corresponding point of a suitably scaled replica of the lower trace in Fig. 1. The number of data points in an FSR was about 370. Under those conditions it was found that an optimum correction for the filter absorption structure could be obtained by means of a computer interpolation algorithm that could effectively shift the filter absorption spectrum by less than one data point interval relative to the spectrum to be corrected. This procedure was tested by restoring the strong quasielastic scattering spectra of several organic liquids, including one, *o*-nitroanisole,²¹ with a width close to that of the observed CP in KTN. The reproduction was not completely faithful near the center of the CP and at the positions of two other prominent I_2 absorptions on the sides. The reason for this is that the I_2 filter absorbs nearly all the light in the ~ 1 -GHz-wide notches at those frequencies.²² The best that can be done in these circumstances is to convolute an *assumed* line shape for the CP with the absorption profiles of the iodine filter and the FP resolution function and proceed to fit the observed spectra. We have applied this

procedure with very good results to the organic liquid spectra and have therefore used it to fit the shape of the CP in KTN with one or two Lorentzian components.

In order to examine the relationship of the CP to the soft TO mode as a function of temperature, the FP was bypassed, and the double monochromator was stepped in increments of 0.24 cm^{-1} with the I_2 filter in place. Since the resolution of the monochromator was 1 cm^{-1} , the CP was not resolved, and convolution procedures were used to fit these Raman spectra. The Raman spectra were also digitally corrected for I_2 filter absorption

III. RESULTS AND DISCUSSION

A. Quasielastic and Brillouin scattering

The Brillouin and quasielastic scattering spectra observed in 90° scattering without the I_2 filter at several temperatures near T_c are shown in Fig. 2. In the region of the sample probed in this set of measurements, the maximum CP intensity is observed at about 37.5 K, which we associate with T_c . Just above T_c , at 39 K, the spectrum consists of the three expected cubic phase phonons, and a background, sloping upwards towards the laser line. This background is the narrowing CP. Note that the phonon peak at about 27 GHz in the 39 K trace is actually a doublet which is well resolved at room temperature. This doublet, together with the weaker line at 45 GHz, account for the three phonons propagating at 45° to the $\langle 110 \rangle$ and $\langle 11\bar{2} \rangle$ axes. The CP intensity increases rapidly below 39 K, and the phonon peaks, particularly the lowest-frequency mode, become shifted and drastically broadened. Below 35 K, the CP rapidly disappears, the lowest-frequency phonon narrows, and the average inten-

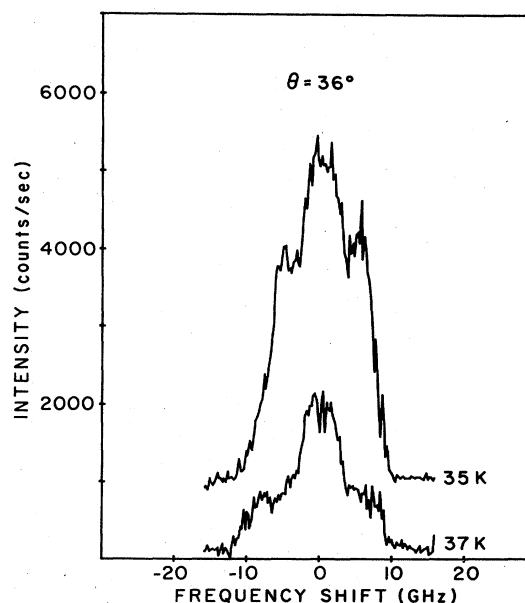


FIG. 4. Central-peak and quasitransverse acoustic phonon observed with a scattering angle of 36° . Phonon intensity is increased by over an order of magnitude by coupling to the overlapping CP. The value of T_c in the sampled region is about 35 K.

sity of the Brillouin peaks is larger by a factor of 3 to 4 compared with $T=39$ K. When a poling electric field is applied along $\langle 111 \rangle$ as the temperature is decreased through T_c , the weak phonon peak at 30 GHz in the 30-K trace disappears, leaving the three phonons that would be expected for a single-domain rhombohedral phase. The characteristics of the quasielastic scattering are not noticeably affected by poling, which suggests that the CP does not simply result from movements of the walls of ordinary, nearly static domains.

The spectra of the quasielastic scattering obtained with 100 mW of laser power at temperatures near T_c using the I_2 filter are shown in Fig. 3. The vertical scales in these traces for which an I_2 filter is employed have been corrected in order to correspond to the scattered intensity that would be observed without the filter. In the range of temperatures shown here the half-width at half maximum (HWHM) of the CP is a minimum between 37 and 38 K, but its shape does not appear to be Lorentzian. The CP intensity near T_c is more than an order of magnitude larger than the strongest Brillouin peak. This situation changes considerably at smaller scattering angles where fluctuations and acoustic phonons of smaller wave vectors are probed. This wave vector $|q|$ varies with the angle θ between the incident and scattered photons as $q = 2nk_l \sin(\theta/2)$, where k_l is the wave vector of the laser light. In order to investigate whether the width of the CP varies with q and to examine qualitatively the effects of coupling between the CP and the lowest-frequency phonon when their intensity distributions are substantially overlapping, spectra were obtained with $\theta=36^\circ$. In the geometry employed q was along $\langle 1\bar{1}0 \rangle$, rather than at 45° to both $\langle 1\bar{1}0 \rangle$ and $\langle 11\bar{2} \rangle$ as in Figs. 2 and 3, and q was

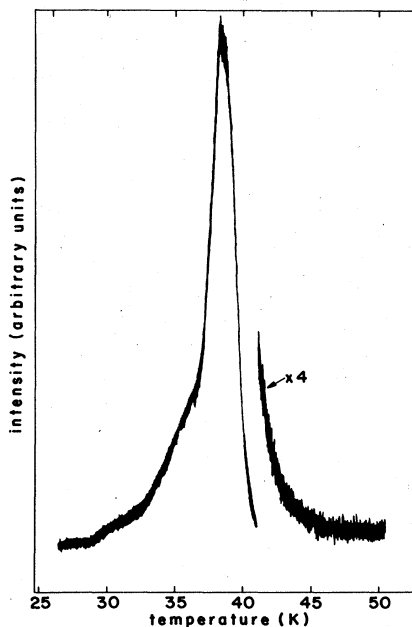


FIG. 5. Integrated intensity of the inelastic central peak as a function of temperature. I_2 filter is inserted and monochromator bandpass is set to 1 cm^{-1} . T_c is at 38 K. The Nb concentration is 3.2 at. %.

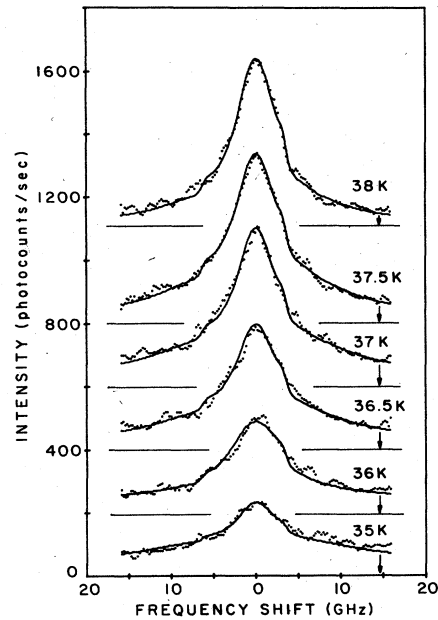


FIG. 6. Reconstructed central-peak spectra fitted to the sum of two Lorentzian functions, as described in the text. The value of T_c is 37.5 K. The HWHM of the fitted curves are $T=38$ K, $\Gamma_1=1.51$ GHz, $\Gamma_2=9.8$ GHz; $T=37.5$ K, $\Gamma_1=1.53$ GHz, $\Gamma_2=10.3$ GHz; $T=37$ K, $\Gamma_1=1.33$ GHz, $\Gamma_2=12.4$ GHz; $T=36.5$ K, $\Gamma_1=1.51$ GHz, $\Gamma_2=12.4$ GHz; $T=36$ K, $\Gamma_1=2.53$ GHz, $\Gamma_2=18.6$ GHz; $T=35$ K, $\Gamma_2=2.9$ GHz; $\Gamma_1=41$ GHz.

reduced by a factor of 0.44. Typical spectra are shown for two temperatures in Fig. 4. Because of the different geometry required for these measurements, a different region of the crystal was probed by the optical system, and the CP was found to have a maximum intensity near 35 K, rather than 37.5 K, as in the $\theta=90^\circ$ data of Figs. 2 and 3. One important aspect of the data of Fig. 4 is that the intensity of the lowest-frequency quasielastic mode is greatly enhanced by about an order of magnitude due to coupling to the overlapping quasielastic scattering peak.

The coupling of the acoustic modes to both the CP and the TO mode is a complicating factor that must be treated carefully in order to obtain a complete understanding of the scattered light spectrum, particularly in the "clamped" limit, that is, for fluctuations of large wave vector for which the acoustic frequencies are smaller than the relaxation rate of the fluctuations. This interesting aspect of the problem cannot be addressed without polarizing scattering measurements on single-domain samples. Fortunately, the uncoupled acoustic phonons have a very low scattering strength when compared to the CP and soft mode, and it is a reasonable approximation to neglect them in dealing with the 90° scattering spectra where the acoustic peaks are in the tail of the narrowing CP near T_c . The plausibility of this statement can be demonstrated by considering the scattered intensity for pairwise-coupled excitations²³

$$S = \sum_{i,j=a,s} F_i F_j \chi_{ij}, \quad (1)$$

where i and j correspond to either of the coupled excitations, the soft mode plus CP (s) or acoustic mode (a), F_s and F_a are their scattering strengths, and the χ_{ij} are the modified susceptibilities given in terms of the uncoupled susceptibilities by

$$\chi_{ii} = \frac{\chi_i^0}{1 - A^2 \chi_i^0 \chi_j^0}, \quad (2)$$

$$\chi_{ij} = \frac{\chi_i^0 \chi_j^0}{1 - A^2 \chi_i^0 \chi_j^0}, \quad (3)$$

where A^2 is the coupling strength which is proportional to an electrostrictive constant times the square of the polarization. Since F_a for the acoustic modes is much less than for the CP or TO phonon, the effects on the CP of the coupling to the acoustic modes involves primarily the denominator of χ_{ss} , which will be most strongly affected near the acoustic peaks where χ_a^0 is appreciable.

Another important property of the small-angle scattering data of Fig. 4 is that the CP width is essentially independent of $|\mathbf{q}|$, the wave-vector transfer, for all temperatures at which it is observable. This excludes the possibility that it arises from "entropy fluctuations" that would be damped by thermal diffusion. Fluctuations of this type would result in a width $\Gamma \propto Dq^2$, where D is the thermal diffusion constant. The lack of such a q dependence is consistent with the apparent absence of any singularity in the heat capacity of KTN near T_c .²⁴

An accurate measurement of the temperature variation of the integrated quasielastic intensity has been made by bypassing the interferometer and detecting only the *inelastic* scattering transmitted through the I_2 filter within the bandpass of the double monochromator centered on the laser frequency. Because the width of the CP is temperature dependent the results of such an experiment depend to some extent on the bandwidth of the monochromator. The results obtained with a 1-cm¹ spectrometer resolution are shown in Fig. 5. These results were obtained by sweeping the sample temperature at a rate of about 0.3 K per minute. The only difference observed when the transition was approached from above or below occurred in the slight undulatory structure in the low-temperature phase. This structure is believed to result from the effects of the sample birefringence on the polarization of the laser beam. It is therefore sensitive to both the detailed domain structure below T_c and to the possible surface depolarization mentioned above. The residual inelastic scattering for $T < 35$ K or $T > 45$ K is caused primarily by the Brillouin components and the weak, broad CP observed by Lyons and Fleury in pure KTaO₃.²⁵ This background has an intensity that increases linearly with increasing temperature. For larger values of the monochromator bandpass, the high-temperature tail of the curve in Fig. 5 is extended to higher temperature. This is consistent with the broadening of the CP for increasing $|T - T_c|$. It is, however, difficult to distinguish between quasielastic scattering and the overlapping vibrational scattering from the TO branch for $T > T_c$ and bandpasses of several cm⁻¹ or more; this is clear from the Raman data presented below.

We now turn to a more detailed consideration of the

shape of the CP. Spectra covering the range of frequency shifts ± 10 GHz are shown in Fig. 6. The procedure discussed in Sec. II was used to convolute an assumed shape function for the CP with the three absorption notches of the I_2 filter that lie in this spectral region and with the instrumental resolution function of the FP. We have used the positions and widths of the I_2 absorption notches measured by Andrews²² for a nearly identical filter operating at the same temperatures as the one employed in the present measurements. The parameters of the shape function were varied to give a best fit to the spectra. Simple Lorentzian functions give poor fits since the observed spectra have a sharp peak superimposed on broad tails. In order to take this characteristic into account, at least qualitatively, the spectra were rather arbitrarily fitted to the sum of two Lorentzian components. These fits are given by the solid lines in Fig. 6. The asymmetric, structured shapes of the calculated spectra are caused by the absorption notches of the filter. The variables in these fits are the maximum intensities I_1 and I_2 , and the half-widths, Γ_1 and Γ_2 , of the two Lorentzian components. The values of Γ_1 and Γ_2 are given in the figure caption. The line shape is consistently fitted by narrow and broad components, both of which decrease in width as T_c is approached from below. These components differ in width by an order of magnitude, and the integrated intensity of the broad component remains about a factor of 2 larger than that of the narrow one over a range of temperatures near T_c . The accuracy of the spectra and the uncertainties in the fitting procedure are such that it is certainly not possible to argue that the quasielastic scattering is fully describable as the sum of two such Lorentzian components. It is clear, however, that the scattering cannot be described by a single Lorentzian and that the quasielastic scattering at frequency shifts greater than a few GHz is characteristic of the broader component, with an apparent HWHM of the order of 1 cm⁻¹.

It should be noted that the non-Lorentzian shape of the CP and the small width of 1.5 GHz (HWHM), a factor of 3 wider than the I_2 absorptions, calls into question to some extent the fitting procedure used here. It may be possible that the CP has a narrower peak of substantial integrated intensity that is not transmitted at all through the I_2 filter. For example, a relaxation process with a distribution of relaxation rates that becomes skewed toward zero near T_c could produce considerable quasielastic scattering that would not be detected in our experiment. That is, the spectra of Fig. 6 may represent the tail of a narrower and more intense peak. It is possible that some of the rounding of the singularity of the integrated CP intensity in Fig. 5 results from such "lost" intensity.

B. Combined optic mode and quasielastic scattering

No first-order Raman scattering is allowed in the cubic phase of KTaO₃. In the ferroelectric phase below T_c , Raman scattering from the soft TO mode is allowed with an integrated intensity given in the mean-field approximation (MFA) by

$$I_T \propto \psi_0^2 \omega_0^{-2},$$

where ψ_0 is the static component of the order parameter

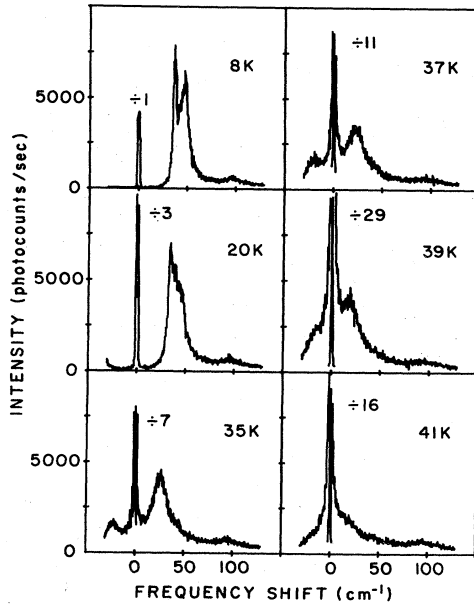


FIG. 7. Reconstructed Raman and central-peak spectra for a range of temperatures near and below T_c . Note the enhancement of the 45-cm^{-1} peak below ~ 20 K. $T_c \sim 39$ K.

and ω_0 is the uncoupled soft-mode frequency. In the MFA, $\psi_0^2 \propto |T_c - T|$ and $\omega_0^2 \propto |T_c - T|^{-1}$, and a step function increase in the integrated intensity would occur at T_c . Order-parameter fluctuations can modify this behavior, however, since $\langle \psi^2(r, t) \rangle$ can be nonzero even when $\psi_0 = \langle \psi \rangle$ vanishes.

The combined quasielastic and Raman scattering have been investigated by resolving the inelastically scattered light transmitted by the I_2 filter with a double monochromator. The monochromator slits were set for a resolution of 1 cm^{-1} . This resolution is, of course, not sufficient to resolve the quasielastic component, and the signal intensity at the laser frequency corresponds, to a good approximation, to the integrated CP intensity transmitted by the I_2 filter. Convolution of the spectra with the monochromator response function allows an investigation of the intensities of the quasielastic and vibrational scattering over a range of temperatures near T_c .

The spectra observed at several temperatures above and below T_c are shown in Fig. 7. The central-peak intensity has been scaled down by the factor indicated in each trace in order to keep it on scale. For the region of the sample probed in these measurements the maximum in the CP intensity occurs at about 39.5 K, about 2 K higher than in Fig. 5. At temperatures below 30 K the contribution to the peak at $\omega=0$ from the quasielastic scattering becomes smaller than the Brillouin scattering. For example, in the trace for $T=8$ K in Fig. 7, only a partially resolved set of Brillouin components is present. Before a further discussion of the CP and TO mode spectra, it is necessary to consider briefly two other scattering processes that complicate the spectra at frequency shifts above about 35 cm^{-1} . Traces obtained at all temperatures, even well above T_c , reveal a background of two-phonon scattering and for $T \gtrsim T_c$ there is disorder-induced scattering from

the TO branch.¹⁶ The intensities of both of these features increase with increasing frequency shift up to the 2 TA peak at about 90 cm^{-1} . There is also a weak feature at about 45 cm^{-1} that appears clearly below T_c , and appears to become enhanced by coupling to the TO_1 mode at the lowest temperatures. It is possible that this feature results from first-order disorder-induced scattering from the TA branch. In order to avoid the extraneous scattered intensity due to these three mechanisms, the spectra of the CP and TO mode will be analyzed only in the frequency region below 35 cm^{-1} where they contribute essentially all of the intensity.

The quasielastic peak and the TO_1 mode scattering both appear quite abruptly below 41 K. The TO_1 mode frequency is about 20 cm^{-1} at T_c and increases to about 40 cm^{-1} at 8 K. Thus, the renormalization of the TO_1 frequency is quite comparable with its value deep in the low-temperature phase. The integrated intensity of the CP and TO_1 scattering near T_c is also comparable with that observed at 8 K.

The simultaneous appearance of the CP and TO_1 scattering and the large renormalization of ω_{TO} near T_c are suggestive of strong coupling between these two excitations. In previous investigations of coupled vibrations and quasielastic or elastic components, a phenomenological form for the combined response function has been employed.^{26,27} This is given by

$$\chi^{-1}(q, \omega) = \omega_0^2(q) - \omega^2 - 2i\omega\Gamma_0 - \frac{i\omega\tau\delta^2}{1 - i\omega\tau} \quad (4)$$

The first three terms on the right-hand side of Eq. (4) are the response function for the uncoupled, damped vibrational mode with frequency $\omega_0(q)$ and damping rate Γ_0 . The fourth term provides coupling of strength δ to a degree of freedom with a Debye relaxation behavior with relaxation time τ . The Stokes scattered one-phonon intensity at ω is proportional to the spectral density

$$S(q, \omega) = \frac{\hbar}{\pi} [n(\omega) + 1] \text{Im}\chi(q, \omega) \quad (5)$$

which is obtained from the fluctuation-dissipation theorem. For sufficiently small values of Γ_0 , it is easily shown that Eq. (5), and its anti-Stokes counterpart with $n(\omega) + 1$ replaced by $n(\omega)$, result in two resolved phonon peaks separated by a central component.²⁷ The renormalized frequency of the phonon is given by

$$\omega_\infty^2(q) = \omega_0^2(q) + \delta^2, \quad (6)$$

and the renormalized width of the central component is

$$\Gamma_c = \tau^{-1} \left[\frac{\omega_0}{\omega_\infty} \right]^2. \quad (7)$$

The relative intensities of the integrated scattering from the central component, I_{CP} and the phonons I_{TO} , varies in the classical limit as

$$\frac{I_{\text{CP}}}{I_{\text{TO}}} = \frac{\delta^2}{\omega_0^2}. \quad (8)$$

As T_c is approached from above or below, $\omega_0 \rightarrow 0$. Then the CP intensity diverges relative to that of the TO pho-

non, and the CP width $\Gamma_c \rightarrow 0$.

Equations (4) and (5) are only appropriate to the case of coupling to a relaxing degree of freedom that has no intrinsic scattering strength in the absence of interaction with the TO phonon. Thus, if the coupled-mode formalism of Eqs. (1)–(3) is employed with $F_{CP}=0$, $F_{TO} \neq 0$, and a response function $\chi_{CP}=i\omega\tau/(1+i\omega\tau)$ is used for the relaxation process, Eq. (4) is obtained. It is not certain *a priori* that this assumption is valid in the present case. Since Eq. (4) has been found to provide a reasonable approximation to the data, however, the results of the computer fits to this formalism will be presented first, and then the necessary assumptions and clarifications will be summarized. Equations (4) and (5) were fitted to the spectra at a number of temperatures. The parameters ω_0 , Γ_0 , δ , and τ and an overall scale factor were varied in order to obtain the best fit to the spectral shape for frequency shifts $-35 \text{ cm}^{-1} < \Delta\omega < 35 \text{ cm}^{-1}$. The calculated one-phonon response, Eq. (5), was convoluted with the monochromator response function, which is broad compared to the CP width. The only property of the CP that strongly affects the fit is, therefore, its integrated intensity. Since the CP is not resolved, the I_2 filter renormalization procedure applied to the spectra of Fig. 7 will not necessarily result in an accurate renormalization of its intensity. An examination of the average attenuation of the I_2 filter over the CP width, measured with the FP interferometer, however, showed it to be within 20% of the attenuation at $\Delta\omega=0$ measured with the double monochromator. Considering the previously mentioned uncertainties regarding unobservable CP intensity lying within the I_2 filter absorption notch, careful corrections for this effect were not considered worthwhile. Below 35 K and above 41 K, the Brillouin components begin to carry a significant fraction of the quasielastic intensity. For this reason the range of temperatures chosen for fitting was $35 \text{ K} < T < 41 \text{ K}$.

The fits to several spectra are shown in Fig. 8, and the resulting parameters are plotted in Fig. 9. The overall scale factor involved in these fits fluctuated by about 10% from 35 to 39 K and decreased rapidly above 40 K. It was not, therefore, a significant variable in fitting the spectra. Although the temperature interval over which the data are fitted is only 5 K, the CP intensity varies by about an order of magnitude. An interplay between the parameters δ^2 and ω_0^2 determines the relative intensities of the CP and the TO_1 phonon wing and also the renormalized frequency ω_∞ , as indicated in Eqs. (6) and (8). Γ_0 fits the shape of the phonon sideband, and τ is only of importance in accounting for the intensity distribution for $\Delta\omega < 5 \text{ cm}^{-1}$. The value of τ^{-1} remained close to 1 cm^{-1} over most of this temperature interval, although it decreased to 0.5 cm^{-1} near T_c , where rounding of the transition caused by Nb concentration fluctuations, lattice strain, or other sources of smearing might be expected to play an important role. The phonon damping rate Γ_0 increased monotonically from 18.5 cm^{-1} at 35 K to 28 cm^{-1} at 40 K.

The fitted values of ω_0^2 decrease linearly to zero at a temperature of about 41 K, which is 1.5 K higher than the value of T_c inferred from the maximum in the CP in-

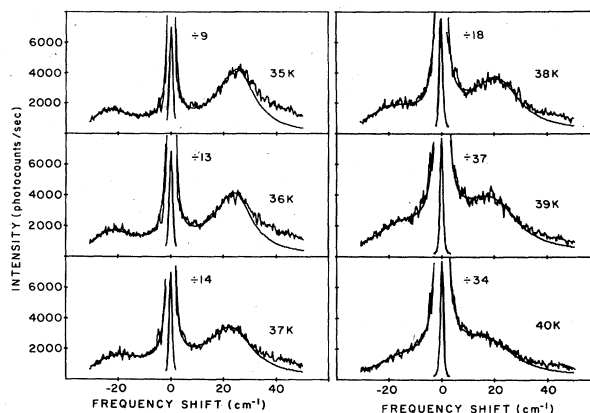


FIG. 8. Optic-phonon and central-peak spectra obtained near T_c ($\sim 39 \text{ K}$). The solid curves are fitted to the spectra using the phenomenological expression for the total susceptibility given in Eq. (4). The scale factors apply to the CP portion of the spectra, where the calculations and the data essentially overlap to within a few percent.

tensity, at 39.5 K in this region of the sample. There are several possible reasons for this difference. The value of $\omega_\infty^2 = \omega_0^2 + \delta^2$ is determined by the shape of the phonon wing, and the ratio δ^2/ω_0^2 is determined by the CP intensity. If there is significant CP intensity that is not transmitted by the I_2 filter and not corrected for by the renormalization procedure, the fitted ω_0^2 will be larger than its actual value. In order to account for the constant upward shift of the ω_0^2 points in Fig. 9, however, the amount of this “missing” intensity must increase rapidly as T approaches 39.5 K. There is no definite evidence that this is the case, although it cannot be discounted in view of the apparently non-Lorentzian shape of the CP.

A second possibility is that the order parameter might be coupled to one or more additional fluctuation mechanisms with very long, or infinite, relaxation times. Impurities, Nb concentration fluctuations, random strains, and dislocations are possible examples. These would cause a very narrow CP that would not be transmitted by the filter. As Lyons and Fleury have noted in their work on lead germanate,²⁸ such a coupling mechanism could be accounted for by adding to Eq. (4) an additional relaxation term of strength δ'^2 and with a very large value of τ' giving

$$\chi^{-1}(q, \omega) = \omega_0^2(q) - \omega^2 - 2i\omega\Gamma_0 - \frac{i\omega\tau\delta^2}{1-i\omega\tau} - \frac{i\omega\tau'\delta'^2}{1-i\omega\tau'} \quad (9)$$

In the limit $\omega \gg \tau'^{-1}$, the results of Eqs. (6)–(8) are altered by replacing ω_0^2 by $\omega_0^2 + \delta'^2$. This would lead to a finite width and a nondivergent intensity at T_c for the observed CP. On this basis, the results of Figs. 8 and 9 could be accounted for by the values $\delta^2 \cong 360 (\text{cm}^{-1})^2$, $\delta'^2 \cong 120 (\text{cm}^{-1})^2$ at 39.5 K. The fact that δ'^2 is somewhat smaller than δ^2 implies that most of the renormalization of the phonon frequency can be accounted for by coupling to the observed CP.

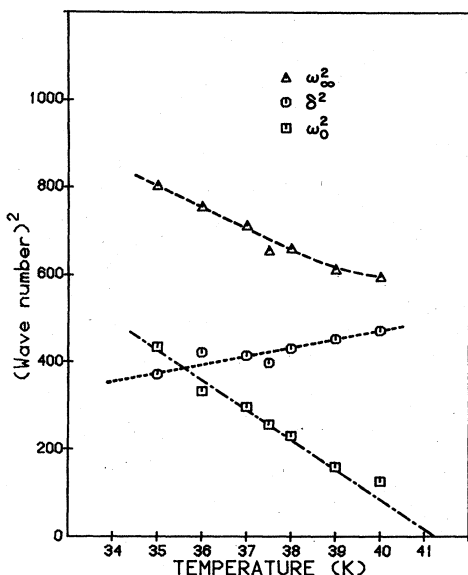


FIG. 9. The fitted values of ω_∞^2 , ω_0^2 , and δ^2 obtained from the spectra of Fig. 8. The lines are drawn as guides to the eye. The Nb concentration is 3.2 at. %.

A remaining source of discrepancy is the smearing of the transition temperature due to Nb concentration gradients, and other sources of inhomogeneity. Because of the very small sample regions probed by the detection optics, we believe that such effects are of importance in a temperature range near T_c that is substantially smaller than the 5-K interval covered in Figs. 8 and 9. In this context it should be noted that the measurements of Fig. 8 were repeated in another region of the sample with very similar results, except for a slightly reduced T_c .

The integrated intensity of the scattering in Fig. 8 has been estimated, and the results are presented as a function of T in Fig. 10. The CP contribution has been estimated by assuming that it has a width characterized by the narrow component [~ 3 GHz full width at half maximum (FWHM)] so that all its intensity lies within the 1-cm^{-1} response function of the monochromator. Since about half its intensity is actually in the broader wing (≤ 20 GHz HWHM), this procedure underestimates its total intensity by a small factor. The intensity variation of the phonon sideband is essentially a step function near T_c . The total intensity of the CP plus phonon sideband, however, has a singular behavior that is not predicted in the MFT.

A final point concerning the Raman data is the applicability of the coupled-mode analysis of Eqs. (4) and (5). Because all Raman scattering is forbidden for $T > T_c$, the observed scattering is caused in lowest order by the fourth-order correlation function of the soft-mode displacement order parameter

$$G_2(r, t) = \langle [\psi(0, 0)]^2 [\psi(r, t)]^2 \rangle.$$

Above T_c this results in two-phonon scattering, and below T_c where $\langle \psi \rangle \neq 0$, both one- and two-phonon scattering

can coexist. Yacoby *et al.*²⁹ have discussed the difficulty of analyzing the resulting superposition of scattering processes, which can include one- and two-phonon interferences. Also, Bruce and Bruce³⁰ have treated quasielastic peaks resulting from two-phonon critical scattering and find that both the inverse width and the intensity of the CP observed in light scattering can have quite different magnitudes and critical behaviors compared to the one-phonon response. In the present case any two-phonon scattering intensity from the soft-mode branch above T_c is very small in comparison with the total scattered intensity observed just below T_c . The two-phonon scattering is unlikely to increase dramatically at T_c , so the assumption that the spectra of Fig. 8 represent the one-phonon response would appear to be appropriate. For this same reason, the use of Eq. (4) to represent the susceptibility of the coupled phonon and CP is justified. The relaxational degree of freedom that causes the CP fluctuations has an unobservable intensity for $T > T_c$ and must derive its scattering strength from coupling to the TO_1 phonon.

C. Origin of the quasielastic scattering

Several properties of the CP and its inferred coupling to the TO phonon sideband are distinctive.

(1) The value of $\delta^2 \sim 400 (\text{cm}^{-1})^2$ is extraordinarily large in comparison with those observed thus far for a nominally displacive phase transition in any pure material. The similar magnitudes of $\omega_\infty^2(T_c)$ and $\omega_\infty^2(0)$ imply that the fluctuations at T_c are comparable to the order parameter at $T \cong 0$.

(2) Measurements of ω_∞^2 at T_c in samples of several compositions imply that δ^2 is a rapidly increasing function of Nb concentration.¹⁶

(3) δ^2 remains finite at T_c .

(4) The non-Lorentzian shape of the CP suggests that there is not a single relaxation time characterizing the fluctuations responsible for the CP.

The known intrinsic sources of central peaks include

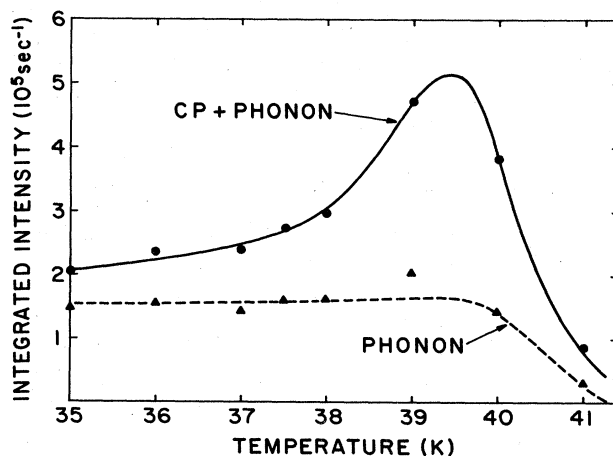


FIG. 10. Integrated intensity of the inelastic scattering of the CP plus phonon wings (solid line) and of the phonon wings alone (dotted line).

both thermal and nonthermal fluctuations, both of which couple to the TO phonon in lowest order through the third-order anharmonicity. The thermal fluctuations, also referred to as entropy fluctuations,³¹ appear to be ruled out here by the lack of q dependence for the CP width. The nonthermal fluctuations, also called "phonon density fluctuations" (PDF), result from two-phonon difference processes.³² A CP resulting from such fluctuations attributed to the flat TA branch exists in KTaO_3 (Ref. 25) and we have also observed it in the KTN samples studied in the present work. There appears to be no reason in principle why such a mechanism could not be responsible for the singular CP observed in KTN, although the property (3) above would imply an inadequacy of the mean-field approximation, which requires that δ^2 vanish at T_c in proportion to $\langle \psi \rangle^2$. A similar behavior has also been found for the singular CP observed at T_c in lead germanate,²⁸ and this behavior was attributed to either higher-order anharmonicity, to the finite- q sampled experimentally, or to fluctuations in the order parameter near T_c . In fact, there is some similarity between the cases of KTN and lead germanate with regard to the CP width, its lack of q dependence, and the finite $\delta^2(T_c)$. The singularity in the CP intensity in KTN is, however, more like that of the elastic CP observed in lead germanate, in addition to the much weaker dynamic CP. Another notable difference between KTN and lead germanate is the non-Lorentzian shape, which would imply coupling to at least two PDF processes with quite different relaxation times.

The characteristics of the CP in KTN that are most difficult to reconcile with an intrinsic mechanism such as a PDF are the large value of δ^2 (about 10^2 larger than in lead germanate) and its dependence on Nb concentration. In view of those properties a CP mechanism involving defect-induced fluctuations caused by the Nb ions seems to be required. In that context a brief summary of the known characteristics of $\text{KNb}_x\text{Ta}_{1-x}\text{O}_3$ is appropriate.

The addition of Nb to KTaO_3 leads to a decrease of the TO_1 soft-mode frequency at temperatures far removed from T_c .^{16,33} This decrease has been attributed to an increased polarizability of the O^{2-} ions surrounding the Nb^{5+} .³³ There are no apparent niobium-induced resonance modes that might imply a local polarization above T_c caused by relative displacements of the niobium and its oxygen ligands. There is, however, evidence for the existence of fluctuations just above T_c associated with Nb. Yacoby¹⁰ has observed Raman activity for the TO_2 "hard mode" above T_c in KTN with $x=0.06$. This result was interpreted on the basis of a mean-field-theory treatment of isolated, displaced Nb impurities. In the view of the present authors, however, the involvement of polarized Nb clusters might also be appropriate in view of the fact that, at $x=0.06$, the mean separation of Nb sites is about two to three lattice constants. Rytz *et al.*³⁴ have analyzed a singularity in the elastic compliance S_{11} of KTN near T_c , again using a mean-field theory that assumes the linear coupling of an unknown defect to the soft mode. This anomaly was fitted for $T > T_c$ to a power law variation of the form

$$\Delta S_{11} = A(T - T_c)^{-\mu}. \quad (10)$$

The resulting values of μ ranged from 1.3 to 1.9, in correspondence with the values expected from the critical exponents appropriate near the "quantum ferroelectric" limit.^{35,36} It is interesting to note that the magnitude of the anomaly decreased with decreasing Nb concentration. The elastic compliance singularity is highly relevant to the quasielastic scattering observed in the present work, since the acoustic anomaly, like the light scattering, is proportional to a fourth-order correlation function of the soft-mode order parameter.³⁷ We have, in fact, fitted the high-temperature tail of the integrated CP intensity shown in Fig. 5 to Eq. (10) by assuming that T_c is given by the position of the maximum. Good fits are obtained for $\mu \cong 1.6$ for a number of sample regions.

Recently, Samara reported measurements of the dielectric constant of KTN with $x=0.02$ under hydrostatic pressure.³⁸ Dispersion is observed above pressures of several kilobars for frequencies on the order of 10^2 – 10^6 Hz. Samara suggests that there is not a ferroelectric phase transition, and the low-temperature "phase" of KTN for $x \sim 0.02$ is a glasslike structure. In the view of the present authors, this conclusion may be in conflict with several optical measurements, such as the abrupt steps observed at T_c in optical depolarization¹⁶ and second-harmonic generation.³⁹ The situation here is perhaps similar to that found in $\text{K}_{1-x}\text{Li}_x\text{TaO}_3$,⁴⁰ for which optical depolarization, vibrational, and acoustic properties have been interpreted as indicating ferroelectric ordering, whereas arguments for a polar glass phase are based on dielectric and nuclear-magnetic-resonance measurements. In any case, it is clear that the reported behavior of the dielectric constant of KTN leaves some doubt as to the exact nature of the low-temperature state at low niobium concentrations. We note, however, that the results of optical depolarization measurements performed in the course of the present work are consistent with the presence of a rhombohedral phase. For example, for light incident along $\langle 100 \rangle$ and polarized along $\langle 110 \rangle$, no depolarization of the transmitted beam is observed. This behavior can be explained only if the optic axes in the low-temperature phase lie along $\langle 111 \rangle$ and equivalent directions. That is because four of the eight possible polar axes are in the plane which is perpendicular to the polarization of the light, which propagates as an ordinary wave in those domains. The other four $\langle 111 \rangle$ axes lie in a plane which contains both the incident wave vector and the polarization vector of the light, and the light propagates as an extraordinary wave in such domains.

The CP spectra presented here provide the first evidence that at least a substantial part of the fluctuation spectrum is distributed over a broad range of frequencies, on the order of $\tau^{-1} \sim 30$ GHz. (It should be noted that this result is consistent with the *absence* of dielectric dispersion at frequencies up to 10^6 Hz in the zero-pressure data presented by Samara.³⁸) This is difficult to reconcile with a model of a small number of isolated impurities or defects which are coupled strongly enough to the order parameter to account for the large value of δ^2 and yet relax on such a short time scale. It seems more likely that the disorder in the unit cell polarizabilities resulting from the random distribution of Nb ions causes polarization

fluctuations having a range of relaxation times due to the varying sizes and configurations of the polarized regions. Qualitative ideas of this type have been proposed by several authors, most of which are reviewed in Ref. 1. In two calculations^{12,41} it has been concluded that the soft phonon frequency will approach a finite limiting value at T_c , $\omega_\infty = \delta$, with δ^2 proportional to the impurity concentration x . This behavior results from the stabilization produced by ordered clusters around the impurities. It is not clear at this time at what concentration, and in what manner, the proportionality between δ^2 and x will be altered at large impurity concentrations.

IV. CONCLUSIONS

An intense, dynamic central peak with a singular intensity increase near T_c has been found in KTN with $x = 0.032$. The coupling of the soft TO_1 mode to the fluctuations causing the observed CP accounts for nearly all of the very sizable frequency renormalization of the phonon. Although phonon density fluctuations cannot be totally excluded as a possible origin of the quasielastic scattering, there are several properties of the spectra and

other experimental results on KTN that provide strong evidence for the involvement of fluctuations produced by the disordered nature of the mixed crystal. Measurements in crystals of different concentrations and for the strain-induced transition in pure $KTaO_3$ (Ref. 42) are in progress and may provide further evidence regarding this possibility. The exact frequency distribution of the fluctuations is at present uncertain. Light scattering measurements at higher resolution and without the I_2 filter are planned in order to investigate this point. If the fluctuations have a narrower distribution than the 1.5-GHz HWHM of the observed CP, strongly dispersive behavior should also appear in the elastic and dielectric response in the sub-gigahertz frequency range.

ACKNOWLEDGMENTS

This work was supported by National Science Foundation Grant No. DMR81-05005. The authors appreciate very useful discussions with P. A. Fleury and K. B. Lyons. Oak Ridge National Laboratory is operated by Martin Marietta Energy Systems, Inc. under Contract No. DE-AC05-840 R21400 with the U.S. Department of Energy.

-
- ¹A. D. Bruce and R. A. Cowley, *Adv. Phys.* **29**, 219 (1980).
²J. B. Hastings, S. Shapiro, and B. C. Frazer, *Phys. Rev. Lett.* **40**, 237 (1978).
³W. Gebhardt and W. Müller-Lierheim, *Proceedings of the International Conference on Lattice Dynamics*, edited by M. Balkanski (Flammarion, Paris, 1978), p. 689.
⁴K. Hisano and K. Toda, *Solid State Commun.* **27**, 915 (1978).
⁵W. Taylor, D. J. Lockwood, and H. Vass, *Solid State Commun.* **27**, 547 (1978).
⁶T. J. Hosea, W. Taylor, and D. J. Lockwood, *Ferroelectrics* **21**, 321 (1978).
⁷Y. Yacoby, *Proceedings of the International Conference on Lattice Dynamics*, edited by M. Balkanski (Flammarion, Paris, 1978), p. 453.
⁸T. Yagi, *Phys. Rev. Lett.* **38**, 609 (1977).
⁹H. Tanaka, *J. Phys. Soc. Jpn.* **44**, 1257 (1978); **44**, 2009 (1978).
¹⁰Y. Yacoby, *Z. Phys. B* **31**, 275 (1978).
¹¹Reference 1 contains a review of the work prior to 1980. Only those treatments directly relevant to this work will be cited here.
¹²B. I. Halperin and C. M. Varma, *Phys. Rev. B* **14**, 4030 (1976).
¹³A. P. Levanyuk, V. V. Osipov, and A. A. Sobyenin, *Theory of Light Scattering in Condensed Matter*, edited by B. Bendow, J. L. Birman, and V. M. Agronovich (Plenum, New York, 1976), p. 517.
¹⁴Y. Imry and S. Ma, *Phys. Rev. Lett.* **35**, 1399 (1975).
¹⁵L. Sasvari and F. Schwabl, *Z. Phys. B* **46**, 269 (1982).
¹⁶R. L. Prater, L. L. Chase, and L. A. Boatner, *Phys. Rev. B* **23**, 221 (1981). Numerous references to previous work on KTN are given in this paper.
¹⁷J. P. Ansermet, D. Rytz, A. Chatelain, U. T. Höchli, and H. E. Weibel, *J. Phys. C* **14**, 4541 (1981).
¹⁸G. E. Devlin, J. L. Davis, L. L. Chase, and S. Geschwind, *Appl. Phys. Lett.* **19**, 138 (1971).
¹⁹K. B. Lyons and P. A. Fleury, *J. Appl. Phys.* **47**, 4898 (1976).
²⁰S. R. Andrews, R. T. Harley, I. R. Jahn, and W. F. Sherman, *J. Phys. C* **15**, 4679 (1982).
²¹G. I. A. Stegeman and B. P. Stoicheff, *Phys. Rev. A* **7**, 1160 (1973).
²²S. R. Andrews, Ph.D. thesis, University of Oxford, 1981.
²³P. A. Fleury, *Commun. Solid State Phys.* **IV**, 167 (1972).
²⁴W. N. Lawless, D. Rytz, and U. T. Hochli, *Ferroelectrics* **38**, 809 (1981).
²⁵K. B. Lyons and P. A. Fleury, *Phys. Rev. Lett.* **37**, 161 (1976).
²⁶F. Schwabl, *Phys. Rev. Lett.* **28**, 500 (1972).
²⁷S. M. Shapiro, J. D. Axe, G. Shirane, and T. Riste, *Phys. Rev. B* **6**, 4332 (1972).
²⁸K. B. Lyons and P. A. Fleury, *Phys. Rev. B* **17**, 2403 (1978).
²⁹Y. Yacoby, R. A. Cowley, T. J. Hosea, D. J. Lockwood, and W. Taylor, *J. Phys. C* **11**, 5065 (1978).
³⁰David A. Bruce and Alastair D. Bruce, *J. Phys. C* **13**, 5871 (1980).
³¹R. K. Wehner and R. Klein, *Physica (Utrecht)* **62**, 161 (1972).
³²R. A. Cowley and G. J. Coombs, *J. Phys. C* **6**, 143 (1973).
³³M. D. Fontana, W. Kress, G. Kugel, N. Lehner, and D. Rytz, *Ferroelectrics* **55**, 23 (1984).
³⁴D. Rytz, A. Châtelain, and U. T. Hochli, *Phys. Rev. B* **27**, 6830 (1983).
³⁵T. Schneider, H. Beck, and E. Stoll, *Phys. Rev. B* **13**, 1123 (1976).
³⁶R. Opperman and H. Thomas, *Z. Phys. B* **22**, 387 (1975).
³⁷U. T. Hochli and A. D. Bruce, *J. Phys. C* **13**, 1963 (1980).
³⁸G. A. Samara, *Phys. Rev. Lett.* **53**, 298 (1984).
³⁹Godefroy Kugel, Hans Vogt, Winfried Kress, and Daniel Rytz, *Phys. Rev. B* **30**, 985 (1984).
⁴⁰See, for example, these most recent articles which give reference to earlier work: B. E. Vugmeister and M. D. Glinchuk,

- Solid State Commun. **48**, 503 (1983); G. A. Smolensky, A. V. Sotnikov, P. P. Syrnikov, and N. K. Yushin, *Ferroelectrics* **54**, 119 (1984).
- ⁴¹H. Schmidt and F. Schwabl, *Phys. Lett.* **61A**, 476 (1977); *Proceedings of the International Conference on Lattice Dynamics*, edited by M. Balkanski (Flammarion, Paris, 1978), p. 748.
- ⁴²Hiromoto Uwe and Tunetaro Sakudo, *Phys. Rev. B* **15**, 337 (1977).